

Supporting Information for

**Lipid spontaneous curvatures estimated from temperature-dependent changes in inverse hexagonal phase lattice parameters: the effects of metal cations**

Marcus K. Dymond<sup>1\*</sup>, Richard J. Gillams<sup>2</sup>, Duncan Parker<sup>2</sup>, Jamie Burrell<sup>2</sup>, Ana Labrador<sup>3</sup>, Tommy Nylander<sup>4</sup>, George S. Attard<sup>2\*</sup>

<sup>1</sup> Division of Chemistry, School of Pharmacy and Biomolecular Sciences, University of Brighton, Brighton, BN2 4GJ, UK

<sup>2</sup> Chemistry, Faculty of Natural & Environmental Sciences, University of Southampton, Southampton SO17 1BJ, UK

<sup>3</sup> MAX IV Laboratory, Lund University, PO Box 118, SE-221 00, Lund, Sweden

<sup>4</sup> Physical Chemistry, Lund University, PO Box 124, SE-221 00, Lund, Sweden

(\*) Authors for correspondence: [M.Dymond@brighton.ac.uk](mailto:M.Dymond@brighton.ac.uk); [gza@soton.ac.uk](mailto:gza@soton.ac.uk)

## Supporting Information for

### SI: 1.0 Method for estimating $c_0$ from the lattice expansion of inverse hexagonal phases

For an elastic deformation with principal curvatures  $c_1$  and  $c_2$  away from the spontaneous curvature  $c_0$  for lipid species  $k$ , the Helfrich free energy (per unit area) is defined as:

$$E_k = \frac{\kappa}{2} (c_{1,k} + c_{2,k} - c_{0,k})^2 + \kappa_G c_{1,k} c_{2,k} \quad (1),$$

where  $\kappa$  is the mean curvature elastic modulus, and  $\kappa_G$  is the Gaussian curvature elastic modulus. Given that for a binary mixture of non-interacting (ideal) amphiphiles (species  $i$  and  $j$ ) the total curvature elastic energy is widely assumed<sup>1</sup> to be a linear combination of the curvature energies of the individual components, such that

$$E_T = x E_i + (1 - x) E_j \quad (2),$$

$E_i$  is the curvature energy of component  $i$ , and  $x$  is its mole fraction.

Assuming that for each species of the mixture  $c_0$  is independent of temperature (i.e. for component  $i$   $c_{0,i}^{(A)} \cong c_{0,i}^{(B)} \equiv c_{0,i}$ ), between the temperatures A and B, the difference in the curvature energy ( $\Delta E_T$ ) gives the following expression:

$$\begin{aligned} \Delta E_T = & \frac{x\kappa_i}{2} \left\{ (c_{1,i}^{(A)})^2 - (c_{1,i}^{(B)})^2 + (c_{2,i}^{(A)})^2 - (c_{2,i}^{(B)})^2 + 2(c_{1,i}^{(A)} c_{2,i}^{(A)} - c_{1,i}^{(B)} c_{2,i}^{(B)}) - 2(c_{1,i}^{(A)} - \right. \\ & \left. c_{1,i}^{(B)} + c_{2,i}^{(A)} - c_{2,i}^{(B)}) c_{0,i} \right\} + \frac{(1-x)\kappa_j}{2} \left\{ (c_{1,j}^{(A)})^2 - (c_{1,j}^{(B)})^2 + (c_{2,j}^{(A)})^2 - (c_{2,j}^{(B)})^2 + 2(c_{1,j}^{(A)} c_{2,j}^{(A)} - \right. \\ & \left. c_{1,j}^{(B)} c_{2,j}^{(B)}) - 2(c_{1,j}^{(A)} - c_{1,j}^{(B)} + c_{2,j}^{(A)} - c_{2,j}^{(B)}) c_{0,j} \right\} + x\kappa_{G,i} \left\{ c_{1,i}^{(A)} c_{2,i}^{(A)} - c_{1,i}^{(B)} c_{2,i}^{(B)} \right\} + (1 - \\ & x)\kappa_{G,i} \left\{ c_{1,j}^{(A)} c_{2,j}^{(A)} - c_{1,j}^{(B)} c_{2,j}^{(B)} \right\} \end{aligned} \quad (3).$$

Since  $c_2 = 0$ , for hexagonal phases, and with the assumption that  $\kappa_i \approx \kappa_j$ ,<sup>2</sup> equation (3) reduces to

$$\begin{aligned} \frac{2\Delta E_T}{\kappa} = & x \{ (c_{1,i}^{(A)})^2 - (c_{1,i}^{(B)})^2 \} + (1 - x) \{ (c_{1,j}^{(A)})^2 - (c_{1,j}^{(B)})^2 \} - 2(1 - x)(c_{1,j}^{(A)} - c_{1,j}^{(B)}) c_{0,j} - \\ & 2x(c_{1,i}^{(A)} - c_{1,i}^{(B)}) c_{0,i} \end{aligned} \quad (4).$$

rearranging in terms of the mixture parameters gives an equation in the linear form:

$$\frac{1}{2} \left\{ (c_1^{(A)})^2 - (c_1^{(B)})^2 \right\} = c_{0\ mix} \left\{ c_1^{(A)} - c_1^{(B)} \right\} + \frac{\Delta E_T}{\kappa} \quad (5)$$

## Supporting Information for

And thus, for a given ideal binary mixture of amphiphiles in an hexagonal phase, a plot of

$$\frac{1}{2} \left\{ \left( c_1^{(A)} \right)^2 - \left( c_1^{(B)} \right)^2 \right\}$$
 against  $\left\{ c_1^{(A)} - c_1^{(B)} \right\}$

for pairs of temperatures (A and B), gives a straight line. The intercept of this line is equal

to  $\frac{\Delta E_T}{\kappa}$  and the slope is equal to the spontaneous curvature of the mixture,  $c_{0 \text{ mix}}$ .

Supporting Information for

SI: 1.1 Lattice parameter data for guest lipids in DOPE host inverse hexagonal phases

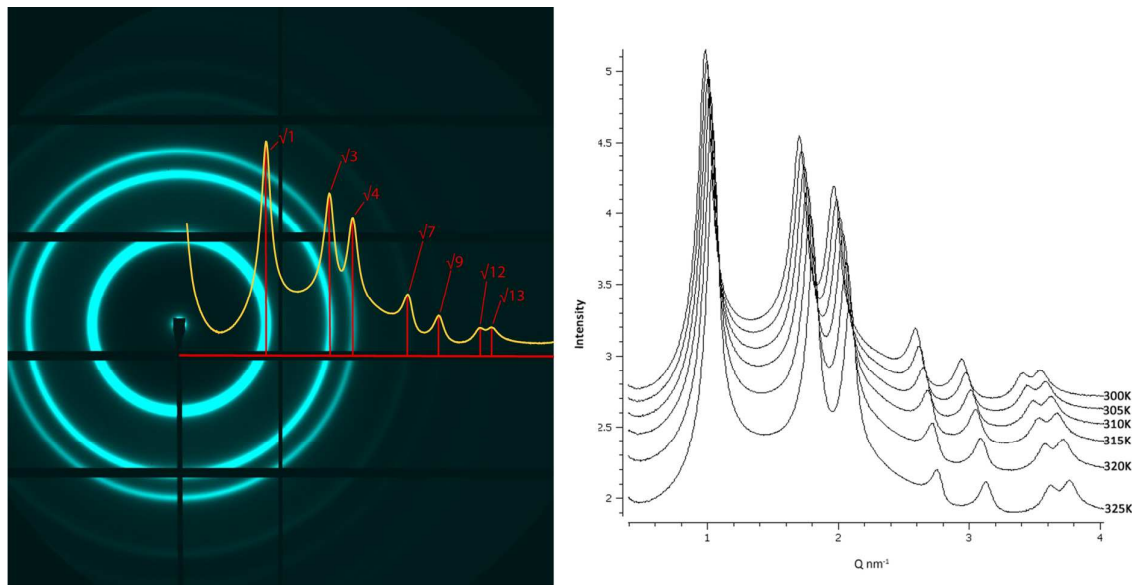


Figure S1 the temperature driven change in  $Q$  of the DOPE inverse hexagonal phase in water.

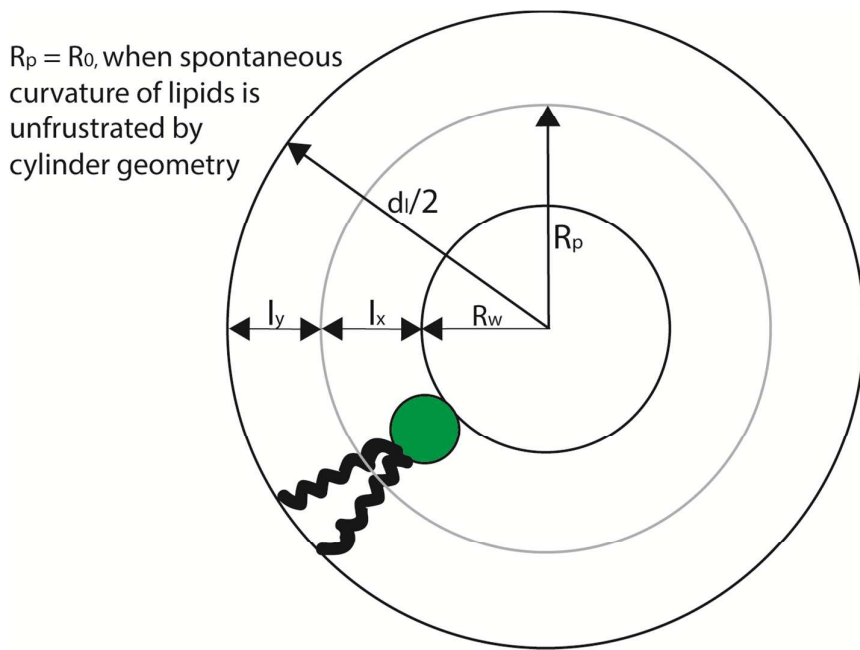


Figure S2 a summary of the relationship between the structural parameters of the inverse hexagonal cylinder and the radii of curvature of planes used to define curvature.  $R_p$  is the radius of the pivotal plane,  $R_w$  is the radius of the water cylinders and  $d_l$  is the interpore spacing (lattice parameter) of the inverse hexagonal phase. The terms  $l_x$  and  $l_y$  describe the individual portions of a lipid of length ( $l = l_x + l_y$ ) split by the pivotal plane.

Supporting Information for

Table S1 lattice parameter data for the host (DOPE)-guest binary lipid mixtures, note in the sample ID W = water, L = low divalent cation concentration  $[M^{2+}] = 13 \text{ mM}$ , M = medium divalent cation concentration  $[M^{2+}] = 65 \text{ mM}$  and H = high divalent cation concentration  $[M^{2+}] = 130 \text{ mM}$ .

Mole fraction DOPA in DOPE	0	0.03	0.06	0.09
Sample ID/ Buffer	PA_0W	PA_3W	PA_6W	PA_9W
	Lattice parameter / nm	Lattice parameter / nm	Lattice parameter / nm	Lattice parameter / nm
<b>TEMP/ °C</b>				
27	7.318367	7.308437	7.2692738	7.377014
32	7.247915	7.244627	7.2085587	7.280694
37	7.147983	7.144941	7.1172455	7.196467
42	7.048634	7.047201	7.0251204	7.100218
47	6.958183	6.958306	6.9413515	7.023572
52	6.907958	6.870255	6.8642198	6.94189
 <b>Mole fraction DOPA in DOPE</b>				
0           0.03           0.06           0.09				
Sample ID/ Buffer	PA_0L	PA_3L	PA_6L	PA_9L
	Lattice parameter / nm	Lattice parameter / nm	Lattice parameter / nm	Lattice parameter / nm
<b>TEMP/ °C</b>				
27	7.377309	7.383698	7.4307481	7.486057
32	7.294723	7.290803	7.3214497	7.391553
37	7.212891	7.192218	7.2282405	7.288659
42	7.119015	7.092867	7.1289138	7.184588
47	7.033387	6.998993	7.0313679	7.102539
52	6.952008	6.907237	6.9473569	7.003717
 <b>Mole fraction DOPA in DOPE</b>				
0           0.03           0.06           0.09				
Sample ID/ Buffer	PA_0M	PA_3M	PA_6M	PA_9M
	Lattice parameter / nm	Lattice parameter / nm	Lattice parameter / nm	Lattice parameter / nm
<b>TEMP/ °C</b>				
27	7.415363	7.405248	7.2079186	7.030101
32	7.327964	7.300216	7.1124913	6.938372
37	7.230668	7.215054	7.0366683	6.852102
42	7.140361	7.110672	6.9531241	6.743155
47	7.049752	7.024761	6.858089	6.662996
52	6.958172	6.925956	6.7864589	6.56156

Supporting Information for

Mole fraction DOPA in DOPE	0	0.03	0.06	0.09
Sample ID/ Buffer	PA_0H	PA_3H	PA_6H	PA_9H
	Lattice parameter / nm	Lattice parameter / nm	Lattice parameter / nm	Lattice parameter / nm
TEMP/ °C				
27	7.464370932	7.418741	7.300553	7.206117
32	7.37591908	7.326673	7.2221116	7.130053
37	7.294245852	7.24318	7.1240395	7.04467
42	7.195232124	7.15134	7.0478415	6.967482
47	7.104148247	7.074437	6.9628076	6.879665
52	7.029605556	6.992024	6.8683479	6.803837
Mole fraction DOPS in DOPE	0	0.03	0.06	0.09
Sample ID/ Buffer	PS_0W	PS_3W	PS_6W	PS_9W
	Lattice parameter / nm	Lattice parameter / nm	Lattice parameter / nm	Lattice parameter / nm
TEMP/ °C				
27	7.318367	7.320729	7.3655772	7.479648
32	7.247915	7.233812	7.2843121	7.394892
37	7.147983	7.140834	7.1908786	7.311123
42	7.048634	7.053119	7.093087	7.206422
47	6.958183	6.959945	7.0099663	7.130331
52	6.907958	6.882221	6.9138694	7.052747
Mole fraction DOPS in DOPE	0	0.03	0.06	0.09
Sample ID/ Buffer	PS_0L	PS_3L	PS_6L	PS_9L
	Lattice parameter / nm	Lattice parameter / nm	Lattice parameter / nm	Lattice parameter / nm
TEMP/ °C				
27	7.377309	7.342283	7.507822	7.70083
32	7.294723	7.279478	7.4262625	7.607004
37	7.212891	7.173369	7.343589	7.511524
42	7.119015	7.082848	7.2449421	7.435543
47	7.033387	7.007373	7.1662438	7.359277
52	6.952008	6.930374	7.0806643	7.27198

## Supporting Information for

Mole fraction DOPS in DOPE	0	0.03	0.06	0.09
Sample ID/ Buffer	PS_0M	PS_3M	PS_6M	PS_9M
	Lattice parameter / nm	Lattice parameter / nm	Lattice parameter / nm	Lattice parameter / nm
TEMP/ °C				
27	7.415363	7.374131	7.3591407	7.19073
32	7.327964	7.286111	7.2853921	7.139247
37	7.230668	7.216116	7.1833717	7.074839
42	7.140361	7.108306	7.0885684	6.991963
47	7.049752	7.032981	7.0020086	6.904628
52	6.958172	6.940901	6.9194905	6.834326

Mole fraction DOPS in DOPE	0	0.03	0.06	0.09
Sample ID/ Buffer	PS_OH	PS_3H	PS_6H	PS_9H
	Lattice parameter / nm	Lattice parameter / nm	Lattice parameter / nm	Lattice parameter / nm
TEMP/ °C				
27	7.464370932	7.419646	7.3885718	7.357927
32	7.37591908	7.356647	7.3187617	7.292476
37	7.294245852	7.290321	7.2351828	7.200502
42	7.195232124	7.159409	7.1352302	7.115207
47	7.104148247	7.092331	7.0399328	7.036205
52	7.029605556	7.009046	6.968704	6.963962

Mole fraction MO in DOPE	0	0.01	0.03	0.06
Sample ID/ Buffer	MO_0W	MO_1W	MO_3W	MO_9W
	Lattice parameter / nm	Lattice parameter / nm	Lattice parameter / nm	Lattice parameter / nm
TEMP/ °C				
27	7.318367	7.319049	7.2590416	7.21647
32	7.247915	7.212133	7.1728754	7.128867
37	7.147983	7.122182	7.0823894	7.03826
42	7.048634	7.040904	6.996525	6.957805
47	6.958183	6.96171	6.9119886	6.876689
52	6.907958	6.868562	6.8206048	6.786829

Mole fraction	0	0.03	0.06	0.09

## Supporting Information for

DiPHYPE in DOPE Sample ID/ Buffer		DiPHY_0W	DiPHY_1W	DiPHY_3W	DiPHY_9W
		Lattice parameter / nm	Lattice parameter / nm	Lattice parameter / nm	Lattice parameter / nm
TEMP/ °C					
27		7.318367	7.188062	7.1037345	7.010862
32		7.247915	7.126846	7.0268301	6.937093
37		7.147983	7.065472	6.9522802	6.864376
42		7.048634	6.973788	6.861591	6.786048
47		6.958183	6.896397	6.7783605	6.709736
52		6.907958	6.815249	6.6990233	6.621081
Mole fraction DD in DOPE Sample ID/ Buffer		0	0.05	0.20	0.30
		DD_0W	DD_5W	DD_20W	DD_30W
		Lattice parameter / nm	Lattice parameter / nm	Lattice parameter / nm	Lattice parameter / nm
TEMP/ °C					
27		7.318367	7.160205	6.7213444	6.137732
32		7.247915	7.066511	6.6535377	6.086439
37		7.147983	6.973425	6.583103	6.012014
42		7.048634	6.873107	6.5174699	5.965222
47		6.958183	6.82305	6.4530165	5.89421
52		6.907958	6.736387	6.3778787	5.850239
Mole fraction HD in DOPE Sample ID/ Buffer		0	0.05	0.20	0.30
		HD_0W	HD_5W	HD_20W	HD_30W
		Lattice parameter / nm	Lattice parameter / nm	Lattice parameter / nm	Lattice parameter / nm
TEMP/ °C					
27		7.318367	7.225091	7.0383737	6.535801
32		7.247915	7.129953	6.9705652	6.46393
37		7.147983	7.033697	6.8798967	6.39424
42		7.048634	6.947037	6.7852082	6.326984
47		6.958183	6.870628	6.6968197	6.273952
52		6.907958	6.790145	6.6131831	6.207613

## Supporting Information for

Mole fraction tRA in DOPE	0	0.06	0.09
Sample ID/ Buffer	tRA_0W	tRA_6W	tRA_9W
	Lattice parameter / nm	Lattice parameter / nm	Lattice parameter / nm
<b>TEMP/ °C</b>			
27	7.318367	7.063724	7.023688
32	7.247915	6.997493	6.930266
37	7.147983	6.939133	6.861241
42	7.048634	6.835805	6.765519
47	6.958183	6.766886	6.69839
52	6.907958	6.686818	6.626895

Mole fraction tR in DOPE	0	0.03	0.06	0.09
Sample ID/ Buffer	tR_0W	tR_3W	tR_6W	tR_9W
	Lattice parameter / nm	Lattice parameter / nm	Lattice parameter / nm	Lattice parameter / nm
<b>TEMP/ °C</b>				
27	7.318367	7.0717212	6.503043	6.405972
32	7.247915	7.0104137	6.479496	6.377027
37	7.147983	6.9357985	6.446094	6.326136
42	7.048634	6.8704673	6.431951	6.288138
47	6.958183	6.7990597	6.39634	6.246173
52	6.907958	6.7231687	6.394455	6.217585

Mole fraction cR in DOPE	0	0.03	0.06	0.09
Sample ID/ Buffer	cR_0W	cR_3W	cR_6W	cR_9W
	Lattice parameter / nm	Lattice parameter / nm	Lattice parameter / nm	Lattice parameter / nm
<b>TEMP/ °C</b>				
27	7.318367	6.9751271	6.584616	6.237239
32	7.247915	6.9168019	6.551888	6.203299
37	7.147983	6.856882	6.519052	6.19719
42	7.048634	6.8093628	6.494948	6.161065
47	6.958183	6.7170249	6.452588	6.144797
52	6.907958	6.6514535	6.432315	6.129206

Mole fraction	0	0.005	0.01	0.03	0.05

## Supporting Information for

### Chol in DOPE

Sample ID/ Buffer	Chol_0W	Chol_05W	Chol_1W	Chol_3W	Chol_5W
	Lattice parameter / nm				
<b>TEMP/ °C</b>					
27	7.318367	7.323842	7.3236703	7.322342	7.265006
32	7.247915	7.254932	7.2344307	7.22784	7.201074
37	7.147983	7.150451	7.1586196	7.130851	7.1085
42	7.048634	7.071813	7.0683478	7.040613	7.020326
47	6.958183	6.957302	6.9821443	6.971696	6.927977
52	6.907958	6.883017	6.8925935	6.864535	6.842135

Supporting Information for

*SI 1.2 Validation of the method of estimating  $c_0$  from the temperature dependence of the lattice parameter of DOPE: anionic lipid mixtures*

To confirm that the changes, we report, in the spontaneous curvature of DOPE: DOPA and DOPE: DOPS mixtures were not artefacts of the method of estimating  $c_0$  we carried out an independent test. For this test we calculated the value of  $c_{0\text{mix}}$  from previously published data<sup>3</sup> that showed the variance of the lattice parameters of inverse hexagonal phases of DOPE: anionic lipid mixtures with temperature, in the presence absence of buffer/divalent cations. Critically, in the published study where we have taken data from, the authors calculate the spontaneous curvature of the lipid mixtures using a traditional method where they reconstruct the electron density profile of hexagonal unit cells. These data are shown in Figures S3 to S5 and clearly show that within experimental error our method reproduces the  $c_0$  values obtained by this traditional method over the composition range, i.e. up to 0.09 mol %, we have studied.

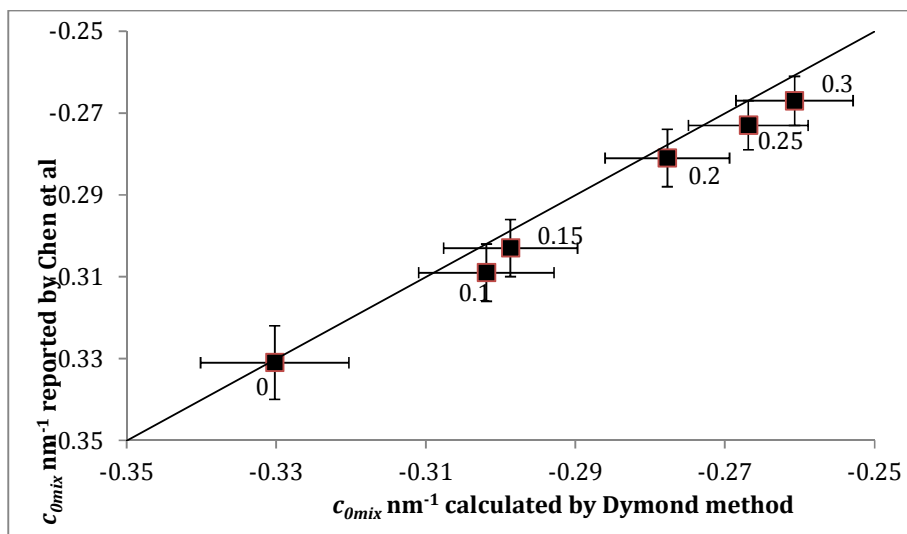


Figure S3 comparing  $c_0$  values of DOPE:DOPA lipid mixtures in water obtained by Chen et al.<sup>3</sup> at 20°C to  $c_0$  values calculated using our method (Dymond et al. method) but using the lattice parameter data published by Chen et al.<sup>3</sup>. The solid diagonal line shows where the two methods give identical results and data labels show the mole fraction of DOPA.

Supporting Information for

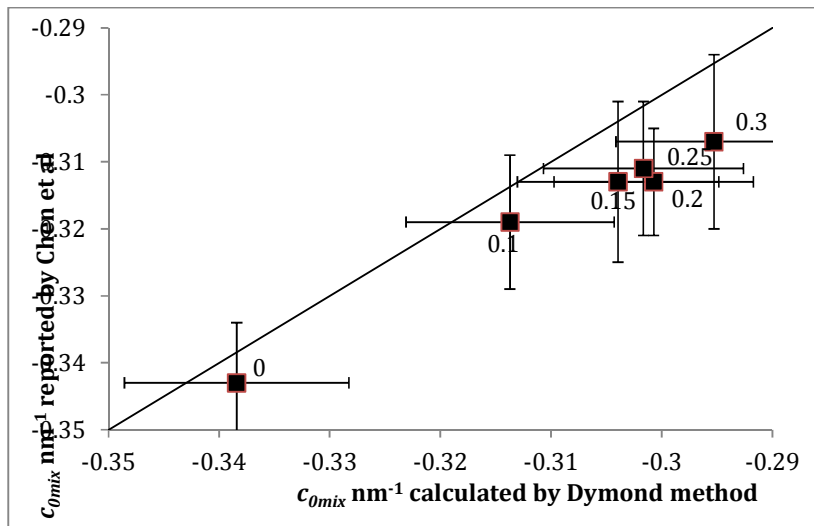


Figure S4 comparing  $c_0$  values of DOPE:DOPA lipid mixtures in 10 mM HEPES, 50 mM  $\text{Ca}^{2+}$  obtained by Chen et al.<sup>3</sup> at 20°C to  $c_0$  values calculated using our method (Dymond et al. method) but using the lattice parameter data published by Chen et al.<sup>3</sup>. The solid diagonal line shows where the two methods give identical results and data labels show the mole fraction of DOPA.

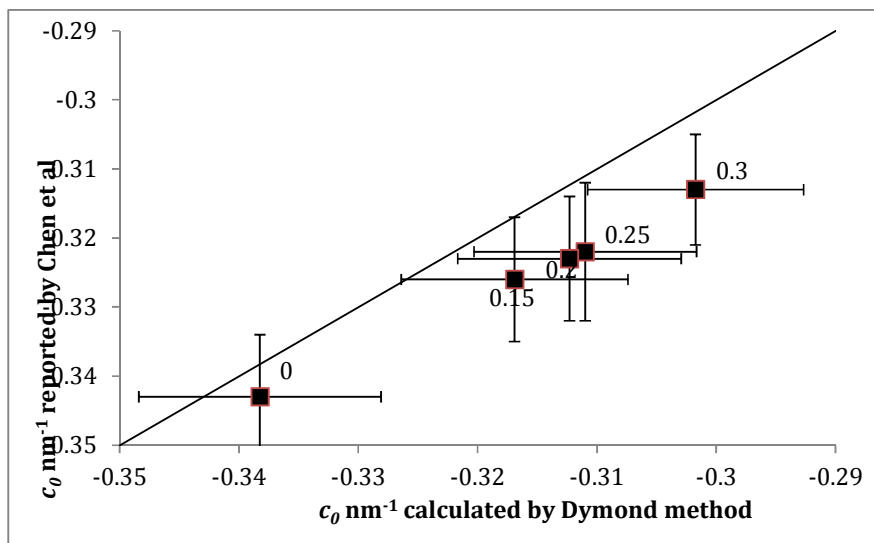


Figure S5 comparing  $c_0$  values of DOPE:DOPA lipid mixtures in 10 mM HEPES, 70 mM  $\text{Ca}^{2+}$  obtained by Chen et al.<sup>3</sup> at 20°C to  $c_0$  values calculated using our method (Dymond et al. method) but using the lattice parameter data of Chen et al.<sup>3</sup>. The solid diagonal line shows where the two methods give identical results and data labels show the mole fraction of DOPA.

Supporting Information for

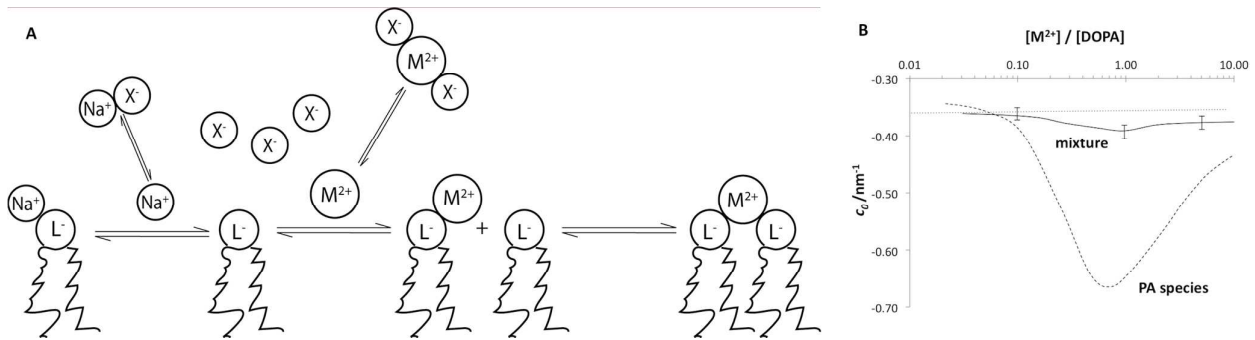


Figure S6A. Schematic representation of the different lipid species that comprise  $c_{0j}$  for a generic anionic lipid ( $L^-$ ) interacting with divalent ( $M^{2+}$ ) and monovalent ( $Na^+$ ) cation salts, where  $X^-$  is a generic salt counterion. These interactions were taken as the basis of the equilibrium model. S6B the total spontaneous curvature ( $c_{0j}$ ) of DOPA (dashed line) as a function of divalent cation concentration, data are determined from the equilibrium association model (Fig S6A) for 9 mol% DOPA such that  $c_{0j}$  of DOPA is sum of multiple lipid species (DOPA-Na, DOPA<sup>-</sup>, DOPA-M<sup>+</sup>, (DOPA)<sub>2</sub>M). The solid curve is the fit to the experimental data for the DOPE: DOPA mixtures i.e.  $c_{0mix}$  versus divalent cation concentration. The horizontal dotted line denotes the value of  $c_0$  for DOPE.

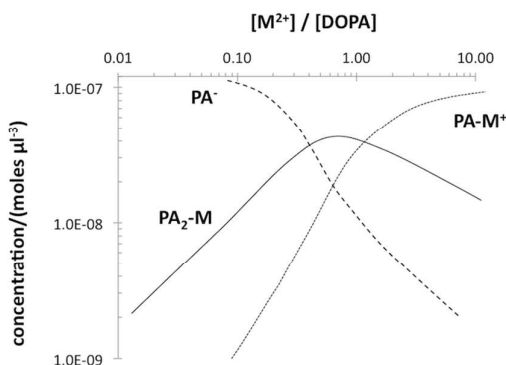


Figure S7. Contribution of individual DOPA lipid species (DOPA<sup>-</sup>, DOPA-M<sup>+</sup>, (DOPA)<sub>2</sub>M) to the spontaneous curvature  $c_{0j}$ , as a function of divalent cation concentration. Data are from the anionic species equilibria model for a lipid concentration of  $4.0 \times 10^{-8}$  moles  $\mu\text{L}^{-1}$  (3 mol% DOPA).

## Supporting Information for

### SI 1.3 Compositional dependence of $c_{0\text{mix}}$ values in DOPE host templates

To confirm that the trends that we observe in our  $c_{0\text{mix}}$  values as a function of the increasing both anionic lipid and divalent cation concentration, shown in Figure 3A and B, are not artefactual we also independently calculated the values of  $c_{0\text{mix}}$  for these samples. This was achieved using the frequently used relationships<sup>3-5</sup> shown in Equations 6 and 7,

$$\phi_w = \frac{2\pi R_w^2}{\sqrt{3}d_l^2} \quad (6)$$

$$R_p = d_l \sqrt{\frac{\sqrt{3}}{2\pi} \left(1 - \frac{V_p}{V_l} \phi_l\right)} \quad (7)$$

Where  $\phi_w$  is the total water volume fraction, and  $\phi_l$  is the total lipid volume fraction,  $d_l$  is the lattice parameter,  $R_w$  is the radius of the water cylinders,  $V_p$  is the lipid volume across the distance  $l_y$  and  $V_l$  is the total lipid volume. Critically since the ratio of  $V_p/V_l$  does not change with up to 30 mol % anionic lipid<sup>6</sup> and its temperature dependence is slight but well detailed<sup>4</sup> we can calculate  $R_p$ , if we know  $\phi_l$  and/ or  $\phi_w$ . We set up our studies above limiting hydration and since there are extensive experimental details in the literature of the limiting hydration value of  $\phi_w$  in DOPE: DOPA and DOPE: DOPS lipid mixtures then using these literature values we can calculate  $R_p$  for our data. We have carried out this calculation using the lattice parameter data we obtained experimentally (Table S1) and compare the answers to those reported in the main document text.

Initially we calculate  $\phi_w$  to assess the extent to which it changes over the range of divalent cation and anionic lipid concentrations studied. We do this for DOPE: DOPS and DOPE: DOPA in water using the published data for the limiting hydration of these lipid mixtures in water. These published data show that in water  $\phi_w$  ranges from 0.27 in pure DOPE to 0.3 in DOPE: DOPA (88:12)<sup>7</sup> and 0.31 in DOPE: DOPA (92:08)<sup>5</sup>, these data show that  $\phi_w$  has a linear dependence compositional dependence with increasing mole fraction of DOPA or DOPS. It is also possible to calculate the values of  $\phi_w$ , using Equation 6, from the work of Chen et al.<sup>3</sup>, who report both  $d_l$  and  $R_w$  for DOPE: DOPA compositions at divalent cation concentrations of up to 100 mM. This calculation shows that  $\phi_w$  has a non-linear relationship with increasing divalent cation concentration and DOPA composition, however the variance is slight ranging from 0.24 to 0.27 with an average and standard deviation of  $0.26 \pm 0.01$ . Since  $\phi_l = 1 - \phi_w$  we calculated the individual values of  $\phi_l$  and used these values in Equation 7, at the divalent cation concentrations that were closest to those used in our studies. Under these conditions the  $R_p$  that emerges from Equation 7 is  $c_{0\text{mix}}$  which we then use to generate the same plot as is shown in Figure 3B. This is shown

Supporting Information for

in Figure S8 where we see the same dependence of  $c_{0mix}$  on  $[M^{2+}]/[DOPA]$ , shown in Figure S6 and similar  $c_{0mix}$  values.

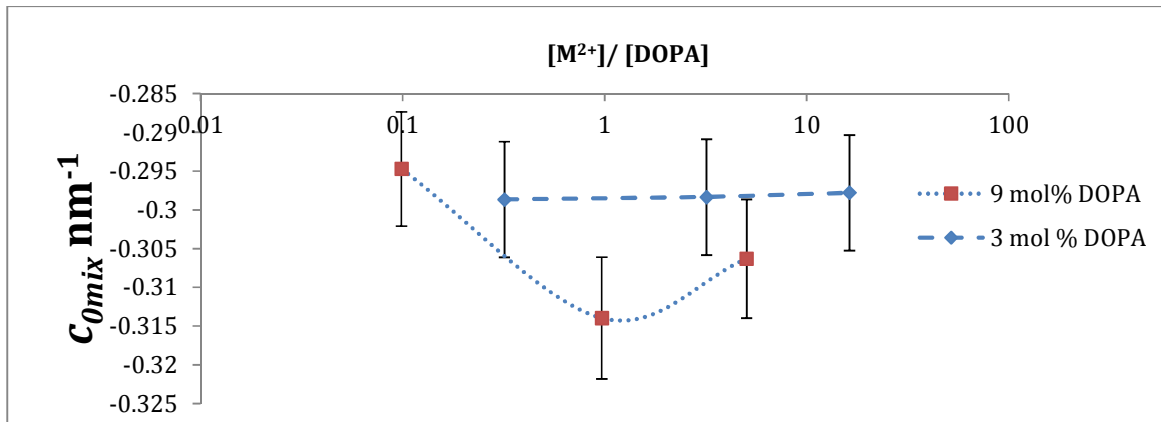


Figure S8 the change in  $c_{0mix}$  with DOPE: DOPA composition and total divalent cation concentration. Data were determined using a ‘traditional’ method to obtain  $c_{0mix}$  as detailed in the SI text and show identical trends to those data in Figure 3A, where  $c_{0mix}$  was determined using our method.

In this context it is interesting to ask what drives this change in  $c_{0mix}$  i.e. changes in  $\phi_l$  or the lattice parameter  $d_l$ . This question is easily answered by setting  $\phi_l$  constant or by randomly varying  $\phi_l$  over the range observed. In both instances the same trend of  $c_{0mix}$  varying with  $[M^{2+}]/[DOPA]$  is seen, which demonstrates that variance in  $d_l$  drives the change we report in  $c_{0mix}$ . In other words changes in  $d_l$  that we observe originate from the change in spontaneous curvature of mixtures and not as artefacts due to our assumption that  $l_y$  does not change significantly with temperature or composition.

Supporting Information for

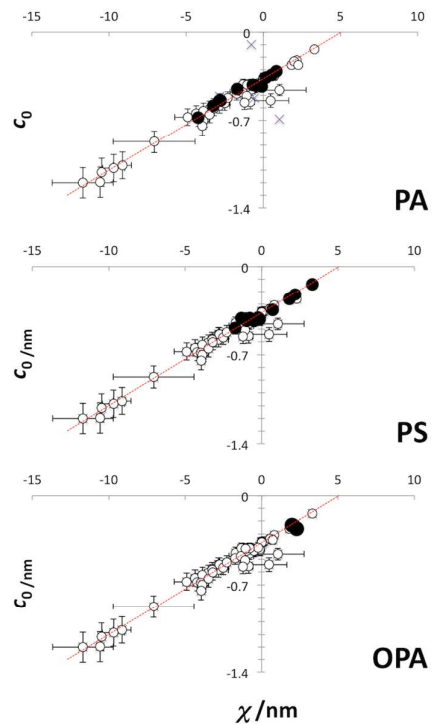


Figure S9. Range of spontaneous curvatures determined from XRD data for the anionic lipids DOPA, DOPS and lysoOPA. Empty, light shaded and dark shaded circles correspond to data for lipid concentrations of  $4.0 \times 10^{-8}$  moles  $\mu\text{L}^{-1}$ ,  $1.3 \times 10^{-7}$  moles  $\mu\text{L}^{-1}$  and  $1.3 \times 10^{-6}$  moles  $\mu\text{L}^{-1}$ .

Supporting Information for

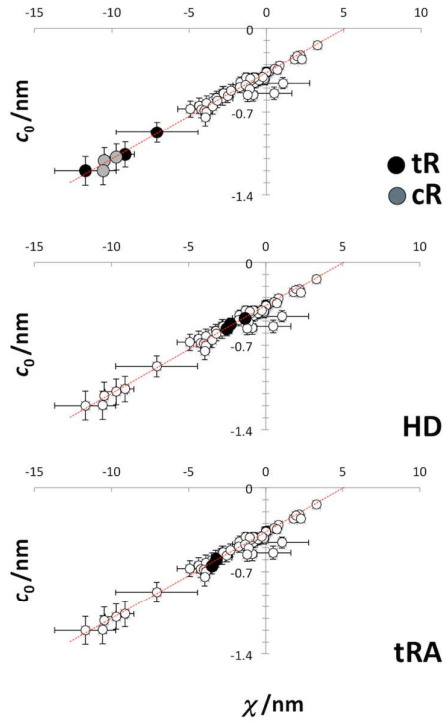


Figure S10. Range of spontaneous curvatures determined from XRD data for the lipids cR, tR, HD and tRA.

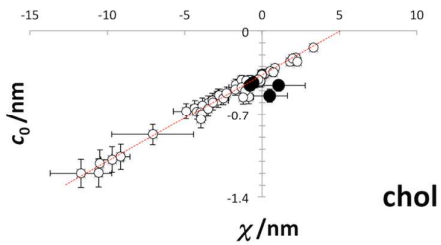


Figure S11 Range of spontaneous curvatures determined from XRD data for the lipid chol.

## Supporting Information for

Table S2, spontaneous curvature data for guest lipids in an inverse hexagonal DOPE host phase; the error in the  $c_{oj}$  or  $R_{oj}$  values is estimated to be  $\pm 7.5\%$ . Where  $Mf_{(j)}$ , is the mole percent fraction of the guest lipid, j, in the host DOPE inverse hexagonal phase,  $c_{o \text{ mix}}$  is the gradient determined from Eq. 1,  $R_o$  is the radius of spontaneous curvature of the guest lipid, j, calculated using our method,  $c_o$  is the spontaneous curvature of the guest lipid, j, and  $\chi_j$  is the curvature power of the guest lipid j, determined from Eq. 7.

lipid j	$Mf_j$ (in DOPE)	$c_{o \text{ mix}}/\text{nm}^{-1}$	$R_{oj}/\text{nm}$	$R_{oj}$ error ( $\pm$ )	$c_{oj}/\text{nm}^{-1}$	$c_{oj}$ error ( $\pm$ )	$\chi_j/\text{nm}^{-1}$	mean $c_{oj}$	sd
chol	0.05	-0.37	-1.84	0.14	-0.54	0.04	0.49	-0.47	0.05
	1	-0.37	-2.18	0.16	-0.46	0.03	1.07		
	3	-0.37	-2.29	0.17	-0.44	0.03	-0.57		
	5	-0.37	-2.20	0.17	-0.45	0.03	0.79		
MO	1	-0.37	-1.79	0.13	-0.56	0.04	-0.86	-0.54	0.03
	3	-0.37	-1.80	0.14	-0.55	0.04	-1.09		
	6	-0.38	-1.98	0.15	-0.51	0.04	-1.22		
diPhyPE	3	-0.38	-1.48	0.11	-0.67	0.05	-4.91	-0.65	0.02
	6	-0.38	-1.55	0.12	-0.65	0.05	-4.35		
	9	-0.39	-1.60	0.12	-0.63	0.05	-3.87		
OA	2	-0.44	-1.46	0.11	-0.69	0.05	-4.00	-0.71	0.03
	3	-0.47	-1.43	0.11	-0.70	0.05	-3.88		
	4	-0.52	-1.34	0.10	-0.75	0.06	-3.98		
cR	3	-0.39	-0.92	0.07	-1.08	0.08	-9.70	-1.13	0.06
	6	-0.41	-0.89	0.07	-1.12	0.08	-10.48		
	9	-0.44	-0.84	0.06	-1.20	0.09	-10.56		
DD	5	-0.38	-1.65	0.12	-0.61	0.05	-3.49	-0.63	0.05
	20	-0.41	-1.71	0.13	-0.58	0.04	-2.82		
	30	-0.46	-1.46	0.11	-0.69	0.05	-3.79		
HD	5	-0.38	-1.91	0.14	-0.52	0.04	-2.29	-0.52	0.04
	20	-0.39	-2.11	0.16	-0.47	0.04	-1.34		
	30	-0.43	-1.77	0.13	-0.56	0.04	-2.51		
tR	3	-0.38	-1.14	0.09	-0.87	0.07	-7.07	-1.05	0.16
	6	-0.42	-0.83	0.06	-1.20	0.09	-11.70		
	9	-0.43	-0.94	0.07	-1.06	0.08	-9.13		
tRA	6	-0.39	-1.53	0.11	-0.65	0.05	-3.19	-0.63	0.04
	9	-0.39	-1.66	0.12	-0.60	0.05	-1.30		

Supporting Information for

Table S3 spontaneous curvature data for guest phospholipids in inverse hexagonal DOPE host phases, we estimate a  $\pm 7.5\%$  error in the  $c_{oj}$  or  $R_{oj}$  values using this methodology. Where  $Mf_{(j)}$  is the mole percent fraction of the guest lipid, j, in the host DOPE inverse hexagonal phase,  $c_{o \text{ mix}}$  is the gradient determined from Eq. 1,  $R_o$  is the radius of spontaneous curvature of the guest lipid, j, calculated using our method,  $c_o$  is the spontaneous curvature of the guest lipid, j, and  $\chi_j$  is the curvature power of the guest lipid j, determined from Eq. 7.

lipid j	[M <sup>2+</sup> ] / mM	Mf <sub>j</sub> (in DOPE)	$c_{o \text{ mix}} / \text{nm}^{-1}$	$R_{oj} / \text{nm}$	$R_{oj}$ error ( $\pm$ )	$c_{oj} / \text{nm}^{-1}$	$c_{oj}$ error ( $\pm$ )	$\chi_j / \text{nm}^{-1}$
DOPE	0	0	-0.37	-2.71	0.20	-0.37	0.03	0.00
	13	0	-0.37	-2.73	0.20	-0.37	0.03	0.00
	65	0	-0.36	-2.74	0.21	-0.36	0.03	0.00
	130	0	-0.36	-2.77	0.21	-0.36	0.03	0.00
DOPS	0	3	-0.37	-2.45	0.18	-0.41	0.03	-0.24
		6	-0.37	-2.88	0.22	-0.35	0.03	0.72
		9	-0.36	-3.85	0.29	-0.26	0.02	1.82
DOPS	13	3	-0.37	-2.43	0.18	-0.41	0.03	-1.32
		6	-0.36	-4.45	0.33	-0.22	0.02	2.18
		9	-0.35	-7.21	0.54	-0.14	0.01	3.31
DOPS	65	3	-0.37	-2.32	0.17	-0.43	0.03	-0.49
		6	-0.37	-2.42	0.18	-0.41	0.03	-0.79
		9	-0.38	-2.04	0.15	-0.49	0.04	-1.73
DOPS	130	3	-0.36	-2.38	0.18	-0.42	0.03	-0.13
		6	-0.37	-2.31	0.17	-0.43	0.03	-0.98
		9	-0.37	-2.39	0.18	-0.42	0.03	-1.04
DOPA	0	3	-0.37	-2.33	0.18	-0.43	0.03	-0.10
		6	-0.37	-2.37	0.18	-0.42	0.03	-0.51
		9	-0.37	-2.95	0.22	-0.34	0.03	0.54
DOPA	13	3	-0.37	-2.39	0.18	-0.42	0.03	-0.69
		6	-0.37	-2.79	0.21	-0.36	0.03	0.16
		9	-0.36	-3.22	0.24	-0.31	0.02	0.84
DOPA	65	3	-0.37	-2.36	0.18	-0.42	0.03	-0.52
		6	-0.38	-1.72	0.13	-0.58	0.04	-3.23
		9	-0.39	-1.47	0.11	-0.68	0.05	-4.21
DOPA	130	3	-0.36	-2.22	0.17	-0.45	0.03	-1.70
		6	-0.37	-1.85	0.14	-0.54	0.04	-2.84
		9	-0.38	-1.85	0.14	-0.54	0.04	-2.77